Colloid Polym Sci (2006) 284: 429–434
DOI 10.1007/s00396-005-1394-2

SHORT COMMUNICATION

Qincui Gu
Keiji Nagai
Mitsuo Nakai
Takayoshi Norimatsu

Polymorphic tin dioxide synthesis via sol–gel mineralization of ethyl–cyanoethyl cellulose lyotropic liquid crystals

Received: 18 April 2005
Accepted: 1 August 2005
Published online: 16 September 2005

Q. Gu · K. Nagai (✉) · M. Nakai
T. Norimatsu
Institute of Laser Engineering,
Osaka University, 2-6 Yamada-oka,
Suita, Osaka 565-0871, Japan
E-mail: knagai@ile.osaka-u.ac.jp
Tel.: +81-6-68798778
Fax: +81-6-68774799

Abstract The polymorphic tin dioxide (SnO_2) was synthesized by calcinating the sol–gel mineralized hybrid of the tin source solution ($SnCl_4$/ethanol/H_2O) and the lyotropic liquid crystal of ethyl–cyanoethyl cellulose((E-CE)C)/acrylic acid (AA). The sub-micrometer SnO_2 spheres with bimodal distribution at 370 and 860 nm were obtained after calcinating the hybrid at 400°C for 5 h. When the hybrid was exposed to ultraviolet first and then calcinated the flying-saucer-like SnO_2 was formed. The exposure time was found to influence the morphology of the as-prepared SnO_2. Except for the spherical and the flying-saucer-like SnO_2, a small amount of well-developed polyhedral SnO_2 was also observed in the as-prepared samples. On this basis, the lyotropic liquid crystal of (E-CE)C/AA afforded a novel route to obtain polymorphic SnO_2.

Keywords (E-CE)C · Lyotropic liquid crystal · Morphology · Sub-micrometer sphere · Tin dioxide

Abbreviations SnO_2: Tin dioxide · (E-CE)C: Ethyl-cyanoethyl cellulose · AA: Acrylic acid · EUV: Extreme ultraviolet · PS: Polystyrene · PMMA: Polymethylmethacrylate · MCF: Macrocellular foam · FE-SEM: Field emission scanning electron microscope · GB: Gentle beam · UV: Ultraviolet · WAXD: Wide angle X-ray diffraction

Introduction

Tin dioxide (SnO_2) has been used for a wide range of technological fields, such as solar cells, gas sensors, lithium battery, separation, catalyst, etc [1–6]. Recently the low-density SnO_2 was proved to be an important laser target material for producing monochromatic extreme ultraviolet (EUV) emission with high conversion efficiency from laser energy [7]. Many techniques including sol–gel, hydrothermal, chemical deposition, magnetron sputtering and microwave irradiation process have been attempted to prepare SnO_2. As the properties of SnO_2 are strongly dependent on its size and shape, it is extremely desirable to be able to exercise size and morphology control during synthesis [8]. Some nanostructural SnO_2, such as nanowire, nanobelt, nanobox, V-shaped, have been prepared by vapor deposition method or chemical synthesis [6, 9–11]. The macrocellular foam (MCF) SnO_2 was obtained through polystyrene (PS), polymethylmethacrylate (PMMA) or silicon colloidal-crystal template method [12–15]. In addition, the sub-micrometer spherical inorganic compounds including SnO_2 are usually prepared through precipitation from corresponding homogeneous solution [16–19]. The as-prepared sub-micrometer spherical metal compounds have been found to consist of small crystalline subunits of about 10 nm. The formation mechanism of sub-micrometer spherical metal compounds such as CdS, Fe_2O_3 etc. is still a topic for discussion and at present the most accepted theory is an aggregation-

of-subunits mechanism [19–21]. In the present work, the anisotropic liquid crystal polymer of ethyl–cyanoethyl cellulose((E-CE)C)/acrylic acid (AA) is adopted to prepare polymorphic SnO_2 including sub-micrometer spheres, flying-saucer-like, etc. To the best of our knowledge, it is the first time to present the polymorphic SnO_2 through the cholesteric lyotropic liquid crystal although the amphiphilic block copolymers were always applied for preparing mesoporous silica [22–24].

Experimental

(E-CE)C (Fig. 1a) was synthesized according to Ref.[25]. AA (Fig. 1b) was purchased from Kanto Chemical. Co. Benzoic ethyl ether from Tolyo Kasei Kogyo Co. Ltd was used as photo initiator for polymerizing AA. $SnCl_4$ with 99.99% purity was obtained from Katayama Chemical Industrial Co. Ethanol (99.5%, Kishida Chemical Co.) was used without further purification. Water was purified by Yamato WG 262 distilling system. Tin source solution was prepared by using $SnCl_4$, ethanol and water according to Ref.[12]. (E-CE)C/AA solution was obtained by mixing (E-CE)C (4.5 g), AA (5.5 g) and the photo-polymerization initiator (0.2 g) and the mixture was kept at room temperature for 1 week. Finally the tin source solution (2 g) was added into (E-CE)C/AA system (8 g) to obtain a hybrid of (E-CE)C/AA/Sn. The hybrid was divided into two parts, one was calcinated at 400°C for 5 h after 1 week's condensation, the other part was firstly exposed to ultraviolet (UV) for 10 or 30 min to polymerize AA, and then the calcination was carried out.

Morphology of the samples was investigated by JEOL JSM-7400F Field Emission scanning electron microscope (FE-SEM) operated at an accelerating voltage of 2 kV in gentle beam (GB) mode. The photographs were recorded by Nikon CCD camera. Photo polymerization of AA was conducted by exposing the samples under UV curing system (UNIDUX Co. Ltd, HX-201E).

Results and discussion

Figure 2 presents the photograph of the (E-CE)C/AA/Sn hybrid with 45 wt% (E-CE)C. The iridescent color indicates a molecular arrangement of cholesteric mesophase when the pitch of the cholesteric helix (referred to as P) is in the optical range. On this basis, the (E-CE)C/AA/Sn hybrid is assessed to be a cholesteric liquid crystal. The color transition from orange to blue is observed along the direction of center to circumference in Fig. 2. The evaporation of the solvent AA results in the color change. From the color distribution, the cholesteric pitch of (E-CE)C/AA was estimated by Huang et al. to be 300–800 nm for 52–42 wt%, respectively [26]. Because the AA evaporation rate in the circumference is faster than that in the center, the solution concentration in the circumference is correspondingly higher and the cholesteric helix should be shorter.

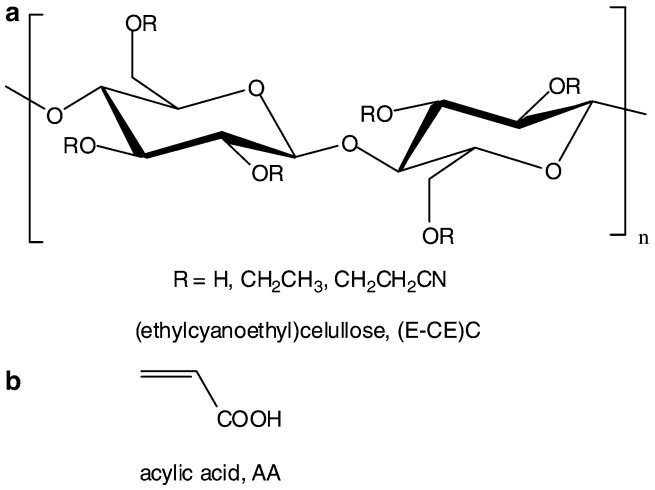

Fig. 1 Chemical structures of ethyl–cyanoethyl celullose [(E-CE)C] (**a**) and acrylic acid (AA) (**b**)

After 1 week's condensation the (E-CE)C/AA/Sn hybrid was calcinated at 400°C for 5 h to decompose the (E-CE)C and other low-molar-mass components. The as-prepared product was confirmed to be SnO_2 by wide angle X-ray diffraction (WAXD) measurement, where sharp diffraction peaks situated at $2\theta \approx 26°$, 33°, 37° and 51° are assigned to the diffractions of ⟨110⟩, ⟨101⟩, ⟨200⟩ and ⟨211⟩ of the cassiterite, respectively . The sub-micrometer SnO_2 spheres with bimodal distribution at 370 and 860 nm are observed under SEM, as presented in Fig. 3a–d. Figure 3a shows that the area of about tens of microns is full of 370 nm SnO_2 spheres and the size distribution scheme given in Fig. 4a indicates the near monodispersity of the spherical particles. The magnified SEM image in Fig. 3b illustrates that the surface of the sub-micrometer spheres is not smooth but like a wool clew, i.e, there is a growth orientation. The SnO_2 nanoparticles of about 10 nm can be discriminated to be a subunit to constitute the oriented wool wires. Except the oriented growth of the subunit, the morphology of the as-prepared SnO_2 is similar to that of metal nickel as reported by Matijevic et al. [27]. As indicated by the arrow in Fig. 3b, the hemispherical SnO_2 is also observed in the view region. It can be judged from the equator face of the hemisphere that the as-obtained SnO_2 is a solid sphere. According to Huang et al., at concentrations of 42–52 wt% (E-CE)C/AA solutions can show a pseudoisotropic texture in some parts of the mesophase. The texture, similar to the planer texture, is

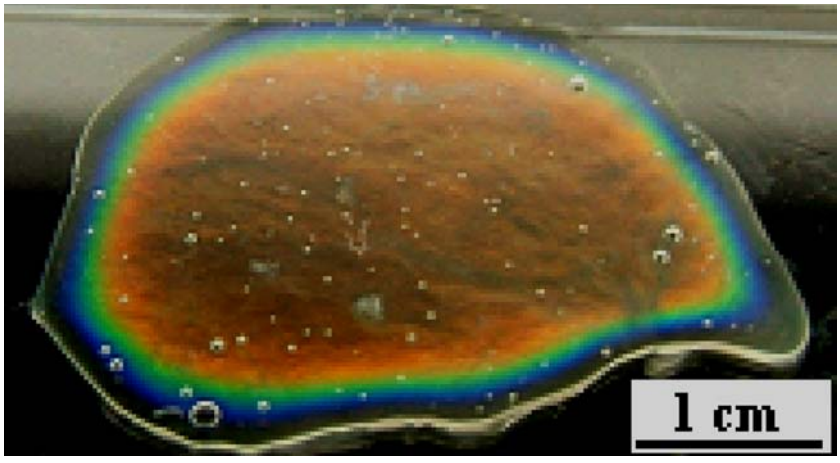

Fig. 2 Photograph of (E-CE)C/AA/Sn hybrid. The weight ratio of (E-CE)C is 45 wt%

a lamellar phase, where the layers of ordered polymer chains are parallel to the solution film plane. The present mono-dispersed sized spheres and hemispheres would be derived from phase separation and be matured between the polymer layers. Except for the small size SnO_2 spheres (370 nm) the big size ones (860 nm) are also found in other area of the same sample, as presented in Fig. 3c. The magnified image in Fig. 3d also illustrates that the SnO_2 nanoparticles of about 10 nm are oriented by means of some law to constitute the sub-micrometer spheres. The monodispersity of the 860 nm spheres is confirmed by the size distribution scheme given in Fig. 4b. The ununiformity of the cholesteric helix pitch of (E-CE)C/AA/Sn hybrid (300–800 nm), depended on position. Main part of center area (orange color in Fig. 2) should be corresponding to large pitch (~ 800 nm) which corresponds ~860 nm spheres. On the other hand, 370 nm particles were mainly observed at the circumference of the picture of which the scale is larger than that of SEM image (Fig. 3a). The SEM image looks like monodispersed spheres, maybe due to very small area in comparison to pitch distribution scale as seen in Fig. 2. Further evidence will be provided to support the speculation.

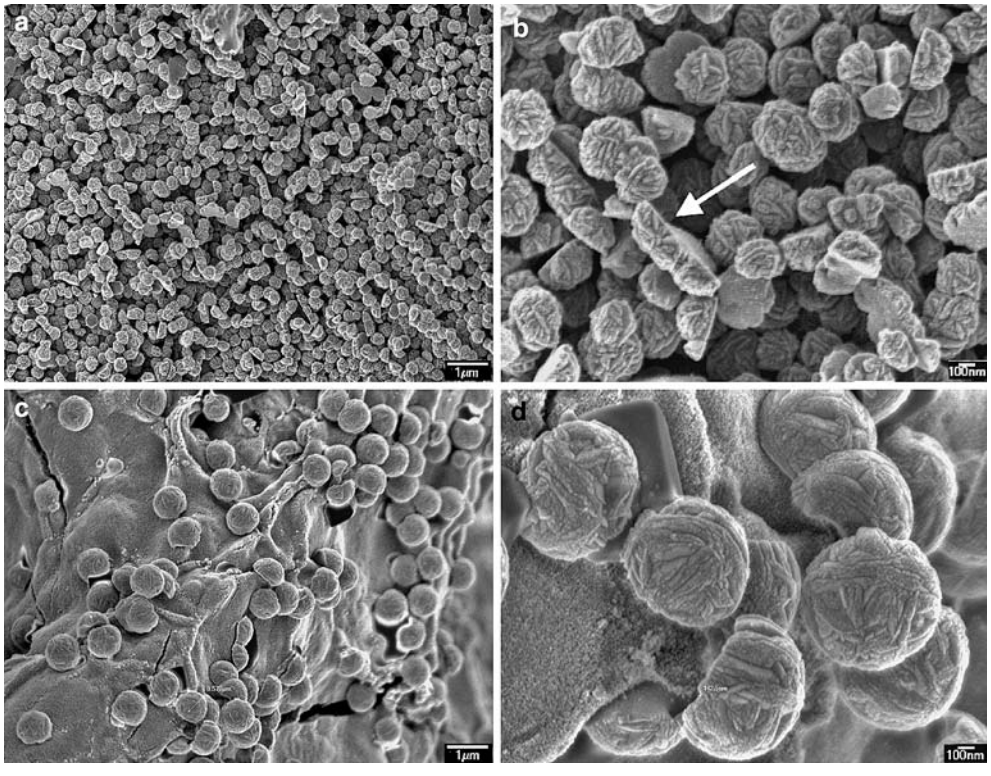

Fig. 3 SEM images of SnO_2 from (E-CE)C/AA/Sn. **a** 370 nm sphere, **b** magnified image of (**a**),**c** 860 nm spheres, **d** magnified image of (**c**)

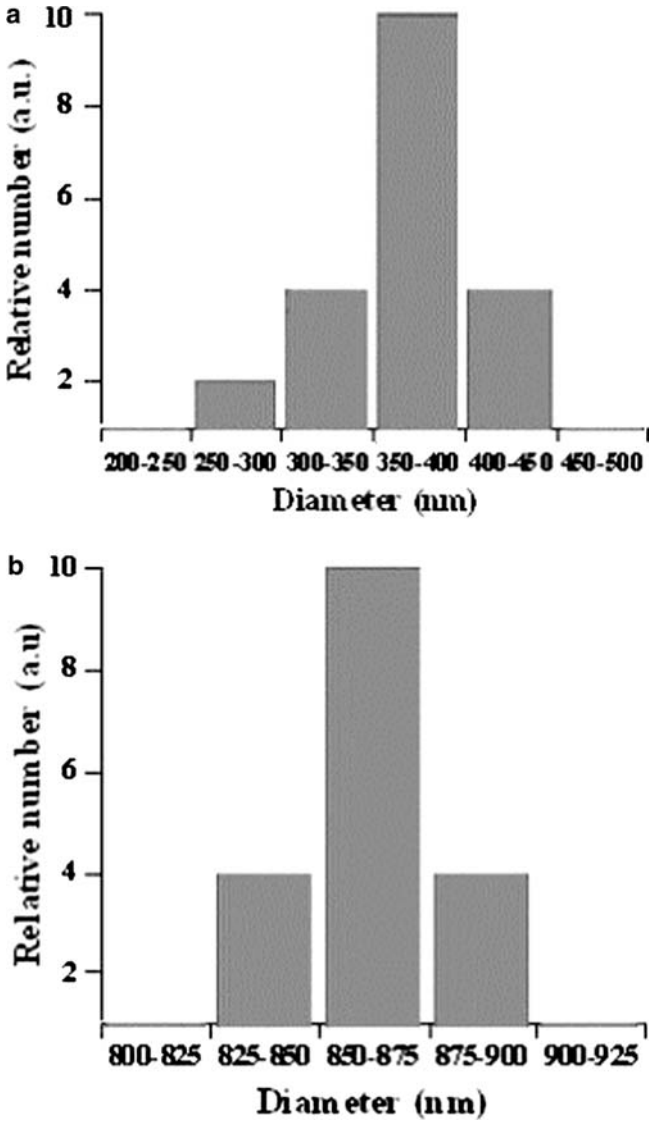

Fig. 4 Histogram of the size distribution of the sub-micrometer SnO_2. **a** small spheres peaked at 370 nm, **b** big spheres peaked at 860 nm

The polymerization of AA is initiated when the (E-CE)C/AA/Sn hybrid is exposed to UV and then the (E-CE)C/AA/Sn is changed to (E-CE)C/PAA/Sn. The polymerization process should affect the morphology of the hybrid more or less, and thus the morphology of the as-prepared SnO_2. The SEM images in Fig. 4a–b describe the morphology of the SnO_2 prepared from the hybrid subjected to UV for 30 min. It can be seen that a flying-saucer-like SnO_2 is obtained instead of sub-micrometer spherical SnO_2. The subunits constituting the flying-saucer-like $SnO_2$is determined to be ~20–30 nm by SEM observation, which is bigger than that of sub-micrometer spherical SnO_2 (10 nm). Therefore, the polymerization affects both the morphology and the subunit size of the as-prepared SnO_2. Similar to the bimodal distribution of the sub-micrometer spheres, the flying-saucer-like SnO_2 are also found to show bimodal sizes at about 340 nm (Fig. 5a) and 800 nm (Fig. 5b) along the long axis direction.

Assuming that the polymerization process is responsible for the formation of the flying-saucer-like SnO_2, the polymerization time must be an important parameter to control the morphology of the as-prepared SnO_2. In order to investigate the effect of the polymerization time, the (E-CE)C/AA/Sn hybrid is exposed to UV for a short time, here 10 min. The SEM images of the as-prepared SnO_2 given in Fig. 6 show that a kind of deformed SnO_2 sphere between sphere and flying saucer was obtained. Therefore, the influence of the polymerization process on the morphology of the as-prepared SnO_2. The polymerization of AA should induce volume shrinkage and pitch shortening of lamellar structure of (E-CE)C/AA. If the shrinkage has an anisotropy due to anisotropic lamellar, the resulted SnO_2 also has anisotropic deformation. When the spherical shape was affected by two dimensional pressure, it should be flying-saucer-like monophology, which can be explained by the anisotropic shrinkage between lamella.

It should be pointed out here that except for the sub-micrometer spheres and the flying-saucer-like SnO_2 a

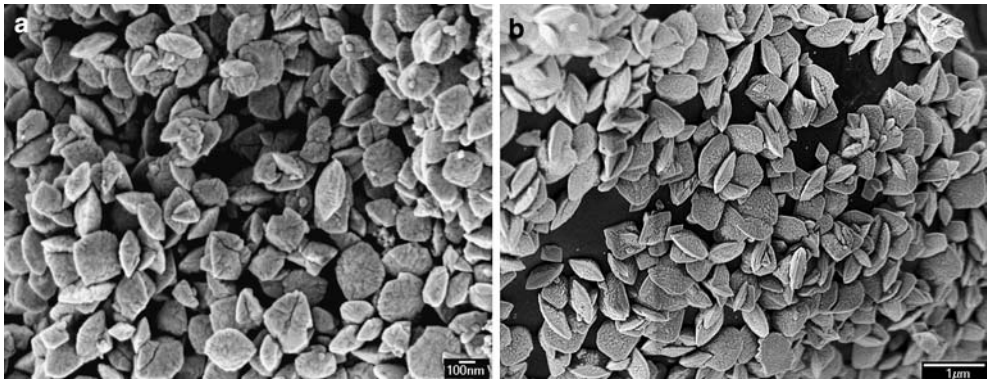

Fig. 5 SEM images of flying-saucer-like SnO_2 from the (E-CE)C/PAA/Sn.**a** 340 nm; **b** 800 nm. (E-CE)C/AA/Sn was exposed to UV for 30 min

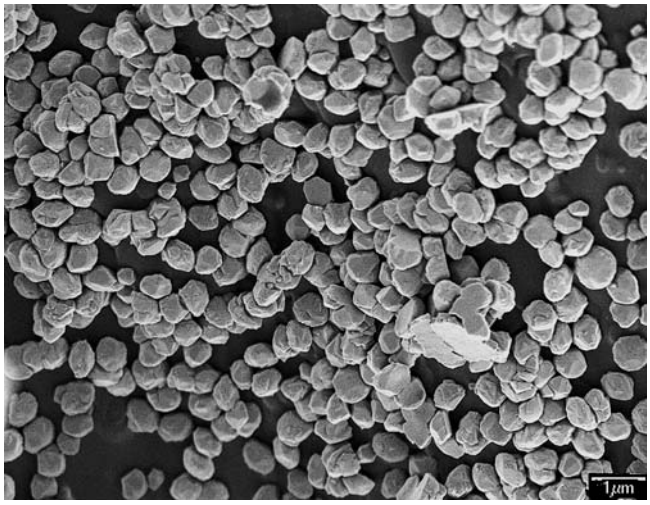

Fig. 6 SEM images of the deformed spherical SnO_2 about 800 nm. SnO_2 was prepared from the (E-CE)C/AA/Sn composite exposed to UV for 10 min

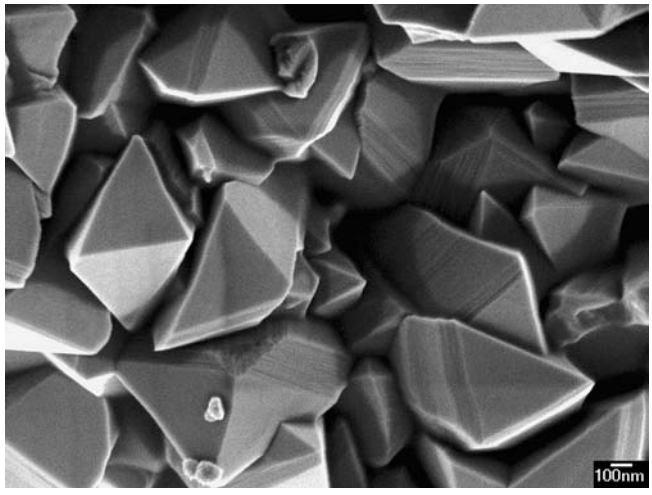

Fig. 7 SEM images of the well-developed polyhedral SnO_2 crystals

small amount of well-developed polyhedral SnO_2 crystals are also observed in the as-prepared sample, as seen in Fig. 7. The size of SnO_2 crystals is in the range of sub-micrometer and detailed observation indicates that the polyhedral crystals are constituted by layered structure. The layer thickness is very uniform and about 10 nm. Although the polyhedral crystalline SnO_2 only occupies a small percentage in contrast to the sub-micrometer sphere SnO_2, it also helps us to plan further experiments to clarify the formation mechanism.

For the application of laser target, low density and sub-micrometer size morphology is required [28–30], while anisotropic morphology is unknown property in laser targets. The present material meets the requirement and provides interesting information depending on the spherical and slightly distorted morphology.

In conclusion, the polymorphic SnO_2 including sub-micrometer sphere and flying saucer was obtained through calcinating the hybrid of the tin source solution and the (E-CE)C/AA lyotropic liquid crystal. The morphological change from sub-micrometer sphere to flying saucer depends on photo-polymerizing the solvent AA or not. Based on the experimental results, the present method provides a novel route to prepare the polymorphic SnO_2 including sub-micrometer one, as it is helpful for clarifying the formation mechanism of the sub-micrometer spherical metal compounds.

Acknowledgements A part of this work was performed under the auspices of MEXT (Ministry of Education, Culture, Science and Technology, Japan) under contract on the subject "Leading Project for EUV lithography source development"

References

1. Wu NL, Tung Chien-Yueh (2004) J Am Ceram Soc 87:1741
2. Schmidt-Winkel PS, Lukens WW, Zhao DY, Yang PD, Chmelka BF, Stucky GD (1999) J Am Chem Soc 121:254
3. Chen FL, Liu ML (1999) Chem Commun 18:1829
4. Ye C, Fang X, Wang Y et al (2004) Chem Lett 33:54
5. Srivastava DN, Chappel S, Palchik O, Zaban A, Gedanken A (2002) Langmuir 18:4160
6. Wang Y, Lee JY, Deivaraj TC (2004) J Phys Chem B 108:13589
7. Nagai K, Nishimura H, Okuno T, Hibino T, Matsui R, Tao YZ et al (2004) Trans Mater Res Soc Jpn 29:943
8. Holmes JD, Johnston KP, Doty RC, Korgel BA (2000) Science 287:1471
9. Jiang X, Wang YL, Herricksb T, Xia YN J (2004) Mater Chem 14:695
10. Zhang DF, Sun LD, Yin JL, Yan CH (2003) Adv Mater 17:1022
11. Liu Y, Dong J, Liu ML (2004) Adv Mater 16:353
12. Gu QC, Nagai K, Norimatsu T et al (2005) Chem Mater 17:1115
13. Lytle JC, Yan HN, Ergang S, Smyrl WH, Stein A (2004) J Mater Chem 14:1616
14. Scott RWJ, Yang SM, Coombs N, Ozin GA, Williams DE (2003) Adv Funct Mater 13:225
15. Sasahara K, Hyodo T, Shimizu Y, Egashira M (2004) J Eur ceramic society 24:1961
16. Gulliver EA, Garvey JW, Wark TA, Hampden-smith MJ, Datye A (1991) J Am Ceram Soc 74(5):1091
17. Barringer EA, Bowen HK (1985) Langmuir 1:414
18. Sondi I, Matijevic E (2001) J Colloid Interf Sci 238:208

19. Libert S, Goia DV, Matijevic E (2003) Langmuir 19:10673
20. Park J, Privman V, Matijevic E (2001) J Phys Chem B 105:11630
21. Libert S, Gorshkov V, Privman V, Goia D, Matijevic E (2003) Adv Colloid and Interf Sci169:100–102
22. Göltner CG, Henke S, Weissenberger MC, Antonietti M (1998) Angew Chem Int Ed 37:613
23. Molvinger K, Quignard F, Brunel D, Boissière M, Devoisselle JM (2004) Chem Mater 16:336
24. Lester CL, Smith SM, Closon CD (2003) Chem Mater 15:3376
25. Huang Y, Chen MC, Li LS (1988) Acta Chim Sin (Chi) 46:367
26. Jiang SH, Huang Y (1993) J Appl Polym Sci 50:607
27. Matijevic E (1981) Acc Chem Rec 14:22
28. Nagai K, Norimatsu T, Izawa Y (2004) J Plasma Fusion Res (Jpn) 80:486
29. Nagai K, Norimatsu T, Izawa Y (2004) Encyclopedia Nanosci and Nanotechnol 10:407
30. Nagai K, Norimatsu T, Izawa Y (2004) Fusion Sci Technol 45:79